ISSN 1590-8844
International Journal of Mechanics and Control, Vol. XX, No. XX, 20XX

CONTROL OF FLOW INDUCED VIBRATIONS BY MEANS OF RESONATORS

A. Doria, E. G. G. Zampieri

Università degli Studi di Padova, Dipartimento di Ingegneria Industriale, Via Venezia 1, 35131 Padova, Italy

ABSTRACT

This paper focuses on flow-induced acoustic vibrations in piping with closed side branches. These self-sustained oscillations can be very violent, causing an unpleasant or harmful noise. In addition, serious mechanical damages to the pipe supports are possible, due to the consequent mechanical vibrations. Since it is often impossible to completely avoid the problem, it is necessary to resort to strategies in order to mitigate its effects, or by shifting the operating conditions in which they can occur towards different frequencies.
This paper deals with the possible use of Helmholtz resonators applied to side branches in order to attenuate noise or to shift the dangerous conditions of resonance. A numerical model is used to study the response of the system in the frequency domain. Initially a side branch with a standard resonator is simulated to highlight the physical phenomena and to study the influence of the main parameters (geometry and position of the resonator).
Then some modifications of the simple resonator are proposed in order to increase the dissipation effects in the neck and improve the attenuation of the acoustic vibrations. In particular, the effect of a helical shaped neck and of a composite neck made up of a bundle of narrow ducts is shown. Finally, the potentialities of a double resonator are investigated.

Keywords: Flow Induced Vibrations, Helmholtz Resonators, Self-Sustained Acoustic Oscillations, Noise Reduction.

1 INTRODUCTION

Flow-Induced Vibrations (FIV) frequently take place in many engineering systems characterized by piping. They can occur whenever there is the simultaneous presence in the piping of flow discontinuities and of specific acoustic resonances. A classic example is represented by junctions between the main pipe (in which the main fluid flux flows) and a side branch closed at the end.
The mechanics underlying excitation has been studied by various authors considering both industrial and aeronautical applications.
Ziada & Lafon [1], as well as Tonon et al. [2], provide an effective picture of the state of the art about this phenomenon. Figure 1 shows that the stable main flow can generate an unstable shear layer due to the presence of discontinuities in the piping.

Contact author:
alberto.doria@unipd.it

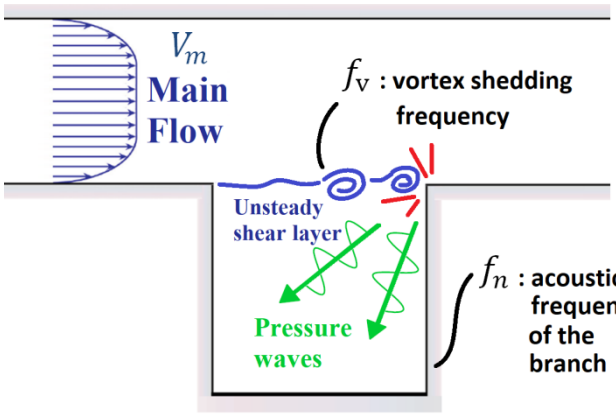

Figure 1: Basic mechanism of the aero-acoustic interaction in a main pipe with a side branch leading to the generation of self-sustained acoustic oscillations.

In particular, when the flow goes beyond the upstream edge of a branch, the dividing line or “shear layer”, that separates it from the stagnant fluid in the closed branch, results highly unstable and easily collapses generating vortices with a certain frequency f_v. The number of vortices along the branch width defines the type of hydrodynamic mode (of the

shear layer) that takes place. These vortices can continue to move along the main pipe or can crash against the downstream edge, giving rise to intense pressure waves which can excite the acoustic resonances of the side branch. If the vortex shedding frequency f_v is tuned to the natural frequencies of the acoustic modes of the side branch f_n (with $n = 1,2,3$ ...), large amplitude pressure waves in the branch can occur (Figure 2), with consequent noise and vibration problems. In particular vibrations cause additional loads on the pipe supports that may lead to possible mechanical damages.

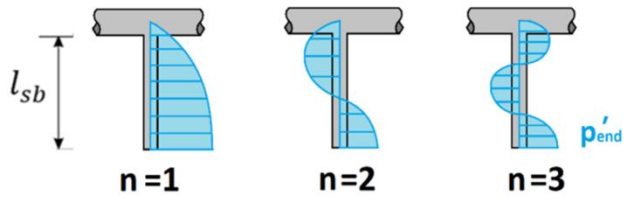

Figure 2: First three acoustic modes of a side branch of a T-junction.

Nowadays, owing to the powerful numerical calculation tools, the acoustic modes of complex pipe systems can be predicted. Conversely, the prediction of the pressure inputs caused by the vortices is still a complex problem, even in case of rather simple geometries.
Given these difficulties, corrective actions must be considered in the piping design to limit the acoustic oscillations. Ziada & Shine [3] developed some design charts to predict the critical flow velocities which show the influence of different geometric parameters, expressed through dimensionless ratios. The oscillations are less intense in long and narrow branches. The effect of the edges in the joint is relevant as well [1]. It was found that rounded edges (the upstream one in particular) increase the instability of the shear layer. Conversely, sharp edges lead to a reduction in the amplitude of the acoustic oscillations. Chamfering the edges can be useful [1] [4], this effect increases the flow velocity at which a resonance may occur and slightly reduces the amplitude of the oscillations. Other suggested control strategies deal with the use of fins [1] [5] positioned in the main pipe in order to maintain the stability of the flow counteracting the flow separation. This solution can lead to a cancellation of the oscillations, but it introduces larger pressure drops. A slightly different strategy is the addition of anti-vortex inserts [1] or simple splitter-plates at the branch inlet [6].
This paper proposes a different approach for controlling FIV of side branches of piping. Since the flow rate, which is related to the main process occurring in the piping, cannot be modified, the acoustic modes of the side branch are de-tuned from the hydrodynamic modes by introducing Helmholtz resonators.
The Helmholtz resonator is a lumped element acoustic device [7] [8] [9] that is successfully used for controlling acoustic oscillations in many machines such as jet engines, combustors, automobile engines, air conditioners and refrigerator compressors.
In recent years the research in the field of Helmholtz resonators focused on devices with particular shape, such as resonators with long neck or deep cavity [10], resonators with extended neck [11] and resonators with helical neck [12]. Many studies on multiple resonators [13] [14] and on Helmholtz resonators liners were carried out as well [15] [16]. Nowadays the development of numerical methods makes it possible to numerically investigate the effect of higher order modes [17] and of geometric details on resonator performance [18].
The paper is organized as follows. In the next sub-section the concept of critical flow speed is introduced. Section 2 deals with the main properties and features of Helmholtz resonators. The numerical model developed in COMSOL is described in section 3. In Section 4 the effect of resonator design parameters on FIV is systematically analysed by means of numerical simulations. Section 5 deals with improved resonators, in which the resonator neck is modified in order to increase damping. The potentialities of a double resonator, which can be tuned to two modes of a side branch, are described in section 6. Finally, conclusions are drawn.

1.1 Critical speed

Experimental analyses carried out by some authors [1] [2] [4] [19] [20] [21] [22] [23] show that the aero-acoustic interaction can be summarized by means of specific diagrams, like the one of Figure 3.

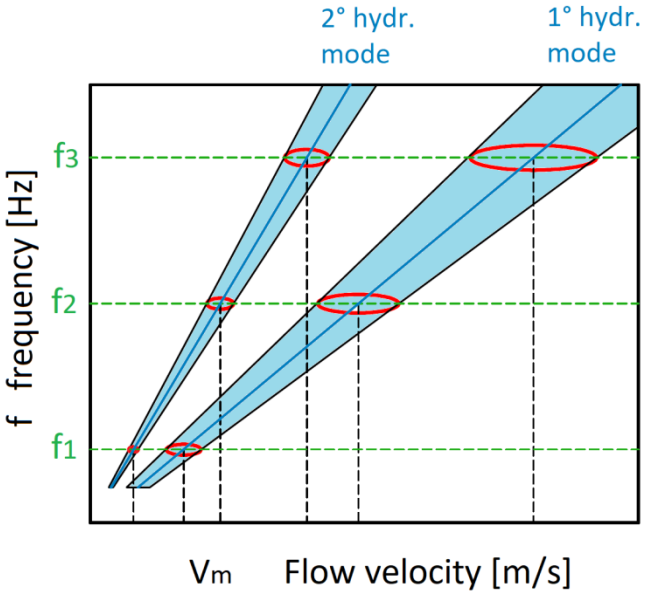

Figure 3: Diagram of aero-acoustic interaction. The red areas indicate the conditions in which large acoustic vibrations are detected.

This kind of diagram synthesizes when the conditions of resonance can take place following more or less the same principle as the well-known Campbell diagram dealing with the critical speeds of rotating shafts [24].

Actually, intense oscillations occur when the frequency of vortices generation (f_v) from the upstream edge of the side branch equals one of the natural acoustic frequencies of the branch itself (f_n). In the diagram this coupling condition is indicated by the crossing between the oblique bands (representing the hydrodynamic modes of the shear layer) and the horizontal lines (representing the acoustic frequencies of the side branch). The latter depend on the type of fluid and on the branch geometry and therefore they can be calculated without difficulty. The simple analytical formula that holds true for a closed side branch is:

$$f_n = \frac{(2n-1)\cdot c_0}{4\cdot l_{sb}} \tag{1}$$

where c_0 is the speed of sound in the gas and l_{sb} is the side branch length and $n = 1,2,3\ldots$ is a positive integer indicating the mode's number. This equation is due to the fact that the acoustic modes (n) of the closed side-branch consist of acoustic standing waves with a pressure node at the junction, a pressure antinode at the closed end and odd multiples of quarter wavelengths in the branch.

The oblique bands in Figure 3, indicate the frequency ranges in which a certain type of hydrodynamic mode takes place (formation of a single vortex, two vortices, or even three vortices) Those ranges are not completely a priori known (since they depend on several factors, including pipeline geometry and operating conditions) however in the literature [3] it is reported that FIV generally occur in typical frequency ranges, which are identified by a dimensionless parameter called the Strouhal number[1]:

$$Str = \frac{f_v \cdot d_{sb}}{V_m} \tag{2}$$

where f_v is the vortex formation frequency, d_{sb} is the side branch diameter (or in general a characteristic length) and V_m is the mean flow velocity in main pipe.

Ziada and Shine [3] found that the excitation related to the first hydrodynamic mode (one vortex) generally happens in a range $Str = 0.3 \div 0.4$. This result holds true considering the simplified case of a side branch sufficiently far from other discontinuities (for example, if the branch is close to an elbow, the range of Strouhal can markedly change). For the second hydrodynamic mode (two vortices) the Strouhal number takes values close to 1.

Peaks of acoustic amplitude of different heights occur by changing the flow speed V_m, when the different resonance conditions due to the aero-acoustical couplings are encountered. Generally speaking, the resonances due to the second hydrodynamic mode are encountered first, because they have a larger Strouhal number.

2 NOISE CONTROL BY MEANS OF RESONATORS

The Helmholtz resonator, which is schematically depicted in Figure 4, is a simple and well known resonating system. It is a lumped element acoustic device that is successfully used for controlling acoustic oscillations in many machines such as jet engines, combustors, automobile engines, air conditioners and refrigerator compressors [2] [8] [9]. In the standard configuration the Helmholtz resonator consists of a cylindrical tube, or neck, open at one end, and connected to a closed cavity at the other end. This simple geometry can be described by just three parameters: the diameter of the neck d_{neck} , the length of the neck l_{neck} and the volume of the cavity V_{cavity} .

The shape of the neck and of the cavity usually do not influence the resonator's behaviour, unless very extreme shapes are adopted [10].

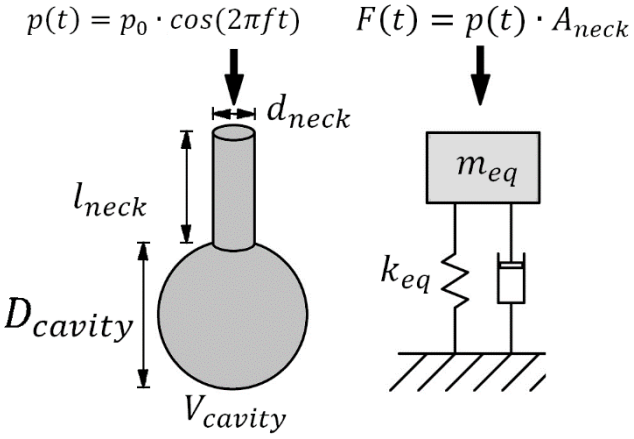

Figure 4: Helmholtz resonator with the equivalent model based on the mechanical-acoustic analogy.

The gas inside the resonator cavity behaves like an elastic element and compresses and extends due to the incoming pressure waves. Conversely, the gas in the neck acts as a rigid mass that moves back and forth. The resonator can be schematized through the mechanical-acoustic analogy (see Figure 4), and the resonance pulsation of the resonator is given by the square root of the ratio between the equivalent stiffness k_{eq} of the elastic element (the gas inside the cavity) and the equivalent mass m_{eq} of the inertial element (the gas in the neck). In formulas these terms are given by:

$$m_{eq} = \rho_0 \cdot A_{neck} \cdot l_{neck} \qquad k_{eq} = \rho_0 \cdot {c_0}^2 \frac{{A_{neck}}^2}{V_{cavity}} \tag{3}$$

where c_0 is the speed of sound in the gas, ρ_0 the density of the gas. Therefore, according to the mechanical-acoustic analogy the natural frequency of a Helmholtz resonator is:

[1] More generally the Strouhal Number is a dimensionless number used in fluid dynamics to describe oscillating flow mechanisms. Its value is given by the ratio between the inertial forces due to the local acceleration of the fluid and the inertial forces due to the convective acceleration.

[2] Their name derives from the German physicist Ferdinand von Helmholtz (1821-1894) even if the general principle of acoustic resonators goes back to the ancient Greeks.

$$f_{res} = \frac{c_0}{2\pi} \cdot \sqrt{\frac{A_{neck}}{V_{cavity} \cdot l_{neck}}} \quad (4)$$

The presence of viscous friction has a small effect on the resonance frequency, but affects damping and the quality factor, which describes the width of the resonance's peak.
For an actual resonator the previous formula can be improved, to take into account that a portion of the gas outside the neck moves with the gas inside the neck increasing in this way the inertial component and causing a significant variation in the resonance frequency. A more accurate expression considering this effect is:

$$f_{res} = \frac{c_{air}}{2\pi} \cdot \sqrt{\frac{\pi \left(\frac{d_{neck}}{2}\right)^2}{V_{cavity} \cdot (l_{neck} + \alpha \cdot d_{neck})}} \quad (5)$$

In which, the length of the neck is increased according to the end-correction α, equal to 0.725 for necks with un-flanged free end, and to 0.85 for necks with flanged end [25].

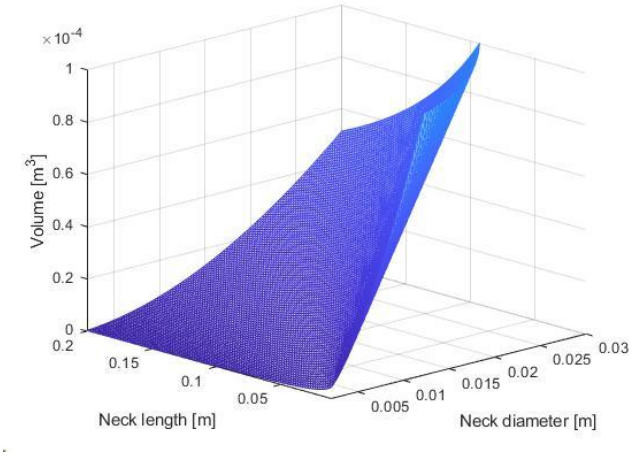

Figure 5: Relationship between the design parameters of Helmholtz resonators with the same frequency.

When the natural frequency of the Helmholtz resonator is assigned, there are ∞^2 combinations of resonator parameters that make it possible to achieve the desired tuning. In geometric terms equation (5) defines a surface in the space that gives one resonator parameter (e.g. V_{cavity}) as a function of the others (e.g d_{neck} and l_{neck}), see Figure 5.

3 NUMERICAL MODEL

The potentialities of Helmholtz resonators in terms of pressure waves attenuation and resonance de-tuning were studied by means of numerical simulations carried out using the software COMSOL.
In order to study the response of the branch as a function of the frequency, a harmonic pressure signal with amplitude 1 Pa and variable frequency was applied at the open end of the side branch. Geometrical models were discretized by means of free tetrahedral elements, an example of mesh is shown in Figure 6. Air at room temperature was considered as the operating fluid.

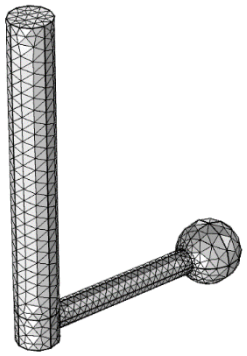

Figure 6: Mesh of the numerical model.

In order to simplify the analysis and identify some tendencies, only one type of junction was chosen. It is a T-junction with sharp edges (see Figure 7) and circular pipes with the side branch having the sizes reported in Table I.

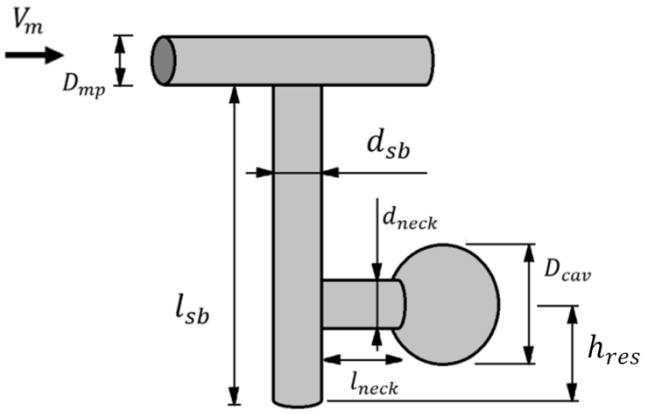

Figure 7: Scheme and characteristic quantities of a T-junction with the applied Helmholtz resonator.

Table I: Reference T-junction sizes.

D_{mp} $[m]$	d_{sb} $[m]$	l_{sb} $[m]$
0.03	0.025	0.2

This side branch has the first three resonances at the frequencies of 429, 1287 and 2145 Hz respectively.

4 SIMPLE RESONATOR

4.1 Side branch with Helmholtz resonator

Numerical simulations and experimental observations show that, if a Helmholtz resonator tuned to one of the acoustic resonances of a side branch is introduced, the corresponding resonance peak disappears in the response spectrum. At the

same time two new peaks appear, the first at a lower frequency and the second at a higher frequency. The heights of the new peaks are lower than the original one due to the friction of the air in the neck of the resonator.

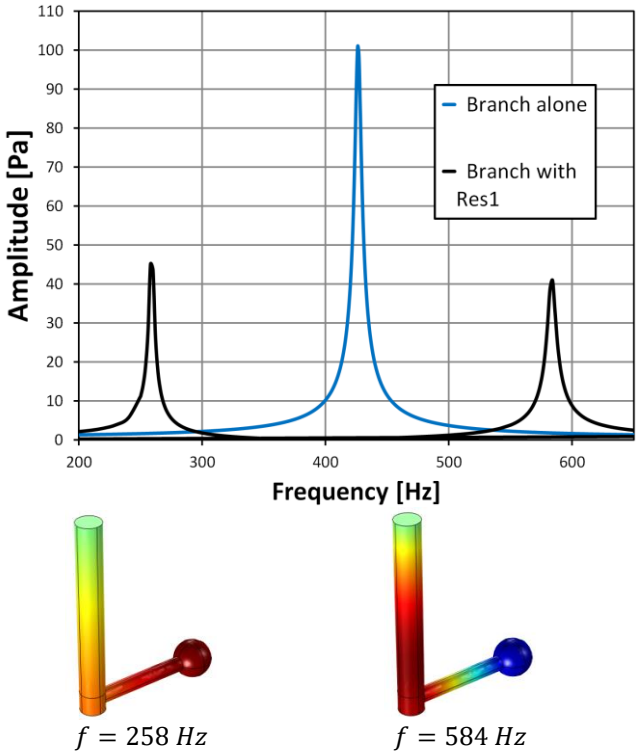

Figure 8: Effect of the application of a Helmholtz resonator (Res1) on the side-branch of the T-junction with the pressure contour plots at the new resonances (red maximum positive pressure, blue maximum negative pressure).

This behaviour is represented in Figure 8, in which the disappearance of the original peak and the appearance of two new lower peaks at different frequencies are evident.
It is worth noticing that the first peak is related to an acoustic mode in which the pressure oscillations in the side branch and in the resonator are in phase. Conversely, the second peak is related to an acoustic mode in which the pressure oscillations in the side branch and in the resonator are in opposition.
The insertion of a standard resonator leads to a decrease in the amplitude of resonance peaks. Moreover, it moves the resonance to different frequencies, moving the dangerous conditions of FIV to different flow speeds. This effect is clear highlighted by the Campbell-like diagram, which is shown in Figure 9. If the two new resonance frequencies (258 and 584 Hz) are considered, the points where they meet the line at Strouhal equal to 0.4 correspond to flow velocities of 16.2 and 36.5 m/s respectively. This means that is possible to operate the pipeline at the velocity of 27 m/s, which initially was considered risky. The danger of FIV is shifted to quite different flow speeds.

In order to exploit in the best way the de-tuning and damping properties of the Helmholtz resonator, parametric analyses are carried out in the next sections.
The position of the axis of the resonator was always set at a distance of 0.01m from the bottom of the side branch.

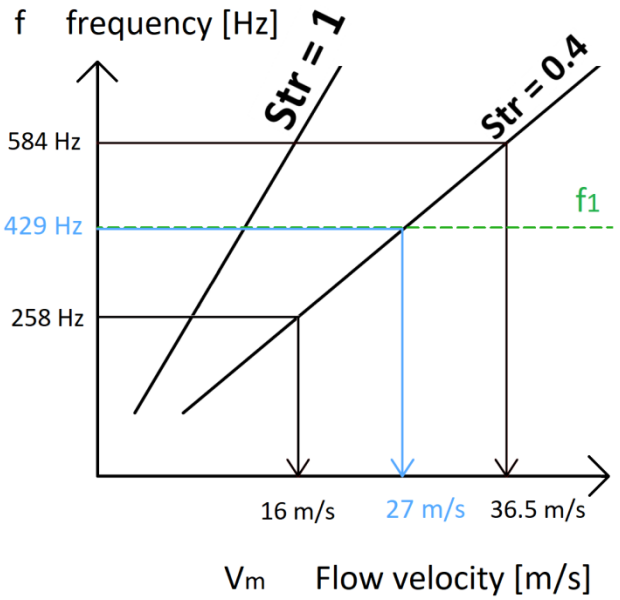

Figure 9: Detuning of the original junction's 429 Hz resonance by applying a resonator, with the new associated flow velocities.

4.2 Resonators with constant neck diameter

The standard configuration of a T-junction with a resonator is shown in Figure 7**.** Four different Helmholtz resonators, each one resonating at the same frequency, corresponding to the first branch-specific resonance (429 Hz) were modelled and simulated. Their features are reported in Table II.
Neck diameter is constant and moving from resonator "Res1" to "Res4" the neck is shortened and the cavity volume is increased according to (5).
The results of this analysis are shown in Figure 10, which represents the transfer function between the acoustic pressure at the closed end of the side branch and the input pressure. The resonator volume influences the height of the first resonance peak but has a very small effect on its frequency. The opposite occurs for the second peak, which can vary a lot in frequency but not in amplitude.

Table II: Sizes of the four Helmholtz resonators used in the simulations and critical speeds.

	d_{neck} $[m]$	l_{neck} $[m]$	V_{cavity} $[m^3]$	$V_{m,1}$ $\left[\frac{m}{s}\right]$	$V_{m,2}$ $\left[\frac{m}{s}\right]$
Res1	0.015	0.088821	$2.87 \cdot 10^{-5}$	16.2	36.5
Res2	0.015	0.07460	$3.35 \cdot 10^{-5}$	16.1	37.5
Res3	0.015	0.06296	$3.88 \cdot 10^{-5}$	15.8	38.3
Res4	0.015	0.04915	$4.77 \cdot 10^{-5}$	15.5	39.7

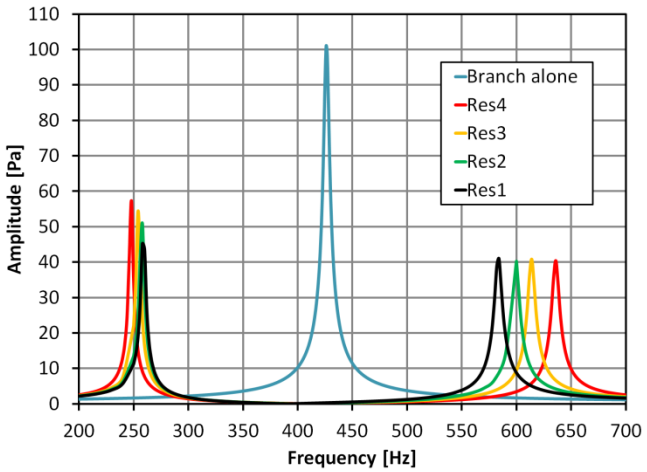

Figure 10: Resonators with constant neck diameter. Effect of cavity volume on the transfer function at the end of the side branch.

The increase in cavity volume leads to an increase in the frequency interval between the two new resonance frequencies. The corresponding critical speeds are reported in Table II.

4.3 Resonators with constant neck length

Four different resonators having the same neck length, but different neck diameters were considered. According to Figure 5 a reduction in neck diameter leads to a reduction in cavity volume as well.

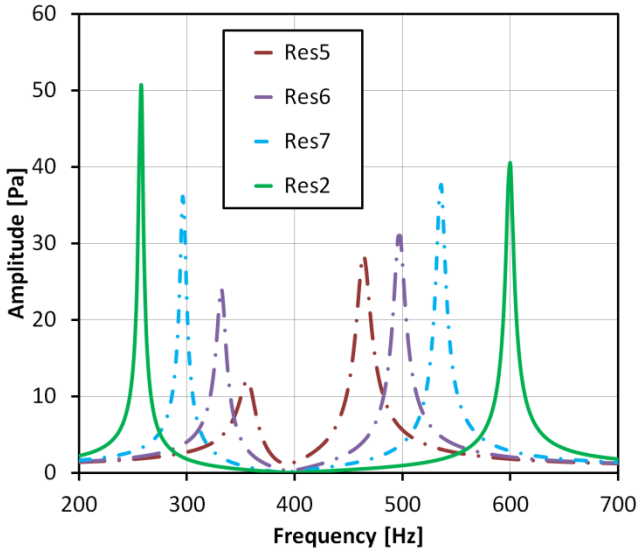

Figure 11: Resonators with constant neck length. Effect of neck diameter on the transfer function at the end of the side branch.

Figure 11 shows that resonators with a very narrow neck and a small cavity generate close and well damped resonance peaks. The small interval between the peaks is due to the small cavity volume. The reduced amplitude in resonance is related to the large friction losses that takes place in a narrow duct. Since the frequency interval between the two new peaks is rather small, a resonator of this type works well if the operating speed (V_m) always remains constant, generating a constant frequency of vortices generation (f_v) at a fixed value between the two resonance peaks.
The critical velocities that correspond to the resonance peaks of Figure 11 are reported in Table III.

Table III: Critical speeds corresponding to the resonance peaks in Figure 11.

	l_{neck} $[m]$	d_{neck} $[m]$	V_{cavity} $[m^3]$	$V_{m,1}$ $\left[\frac{m}{s}\right]$	$V_{m,2}$ $\left[\frac{m}{s}\right]$
Res5	0.0745	0.004	2.62E-6	22.2	29.0
Res6	0.0745	0.0065	6.78E-6	20.7	31.1
Res7	0.0745	0.01	1.55E-5	18.5	33.5
Res2	0.0745	0.015	3.35E-5	16.1	37.5

4.4 Resonators with constant cavity volume

The parametric analysis was completed considering a set of resonators with constant volumes and different neck lengths. A decrease in neck length required a contemporary decrease in neck diameter to keep constant the resonance frequency.

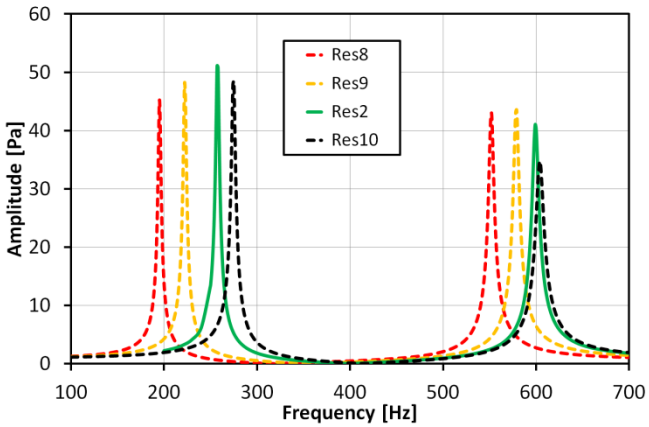

Figure 12: Resonators with constant cavity volume. Effect of neck length on the transfer function at the end of the side branch.

Results, which are represented in Figure 12, show that a decrease in neck length causes a shift of both resonance frequencies towards higher values. This result is in agreement with physical intuition, since a decrease in the sizes of the neck decreases the equivalent mass (equation (3)) and may lead to an increase in the natural frequencies of the coupled system.
The effect of neck geometry on the height of the resonance peaks is less clear. On the one hand the decrease in neck length decreases friction losses, on the other hand the decrease in neck diameter increases friction losses.
Also in this case the corresponding critical velocities are shown in Table IV.

Table IV: Critical speeds corresponding to the resonance peaks in Figure 12.

	V_{cavity} $[m^3]$	l_{neck} $[m]$	d_{neck} $[m]$	$V_{m,1}$ $[m/s]$	$V_{m,2}$ $[m/s]$
Res8	3.35E-5	0.1842	0.023	12.1	34.5
Res9	3.35E-5	0.1354	0.02	13.8	36.1
Res2	3.35E-5	0.0746	0.015	16	37.4
Res10	3.35E-5	0.0307	0.01	17.2	37.7

4.5 Effect of resonator position

Possible effects of the position of the resonator (considered as the distance of the axis of the neck from the closed end of the branch) on the acoustic oscillations were also investigated.

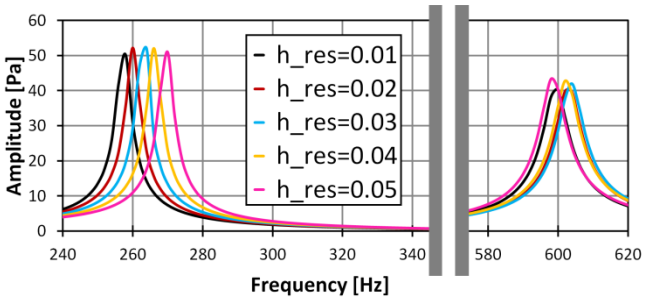

Figure 13: Effect of resonator position.

Five different simulations were carried out in which the resonator "Res1" was considered. Its initial position was at a distance of 0.01m from the closed end of the branch and was then varied each time by 0.01m, up to 0.05 m. Figure 13 shows that the position has a very small influence on oscillations amplitude.
Also the frequencies vary only slightly, the first more regularly, increasing when the distance increases.
These results can be understood considering that the simulated displacements do not strongly modify the coupling between the resonator and the side branch mode, which is the 1/4 wave-length mode.

5 MODIFIED RESONATORS

In this section the study is extended considering non-standard resonators with modified geometry, in order to improve their performance. To obtain highly damped peaks it is necessary to increase the friction in the neck. A resonator with helical neck (Figure 14) can achieve this result [26].
The effect of this shape was studied considering two resonators, the former with a standard straight neck, the latter with an equivalent neck that makes a helix turn (and having the same diameter of the neck and the same cavity volume). The resonator with helical neck considered in this simulation is described in Table V.

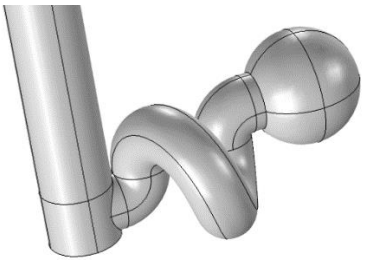

Figure 14: Model of the resonator with helical neck.

Table V: Dimensions of the resonator with helical neck.

	d_{neck} $[m]$	D_{cavity} $[m]$	Pitch p $[m]$	Radius r $[m]$	$V_{m,1}$ $\left[\frac{m}{s}\right]$	$V_{m,2}$ $\left[\frac{m}{s}\right]$
ResH	0.02	0.04	0.03	0.016	14.1	37.4

Numerical results, which are depicted in Figure 15, show that the helical resonator has the resonance peak related to the second mode moved to higher frequencies compared with the standard resonator. Moreover, the amplitude of the resonance peaks decreases, especially for the first mode. This effect is due to the increased losses in the neck caused by the helical geometry. Finally, this solution makes it possible to realize more compact resonators requiring less space despite having the same desired frequency.

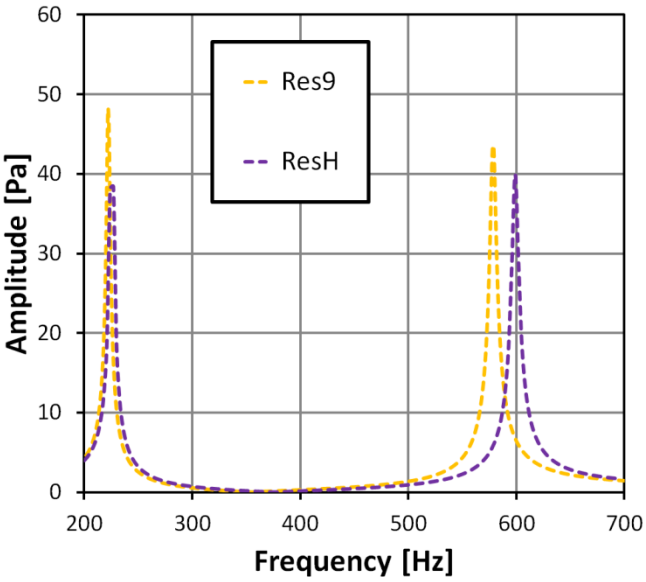

Figure 15: Effect of the adoption of a resonator with helical neck.

A further solution was conceived dividing the neck into a series of parallel necks globally having the same cross section of the standard neck. This solution leads to an increase in the friction of the air in the neck due to the larger contact surface on which the air slips at each oscillation.
To analyse the potentialities of this concept, some simulations were carried out by dividing the neck into four (Figure 16) and eight smaller tubes.

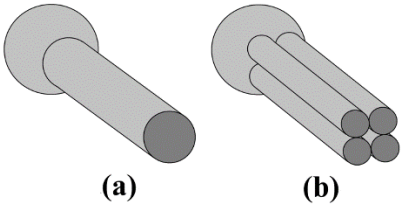

Figure 16: Standard resonator (a) and equivalent resonator obtained by substituting the neck with a bundle of tubes (b).

The results are shown in Figure 17. The division of the neck into several parts generates larger losses and there is a significant reduction in the height of the resonance peaks. The resonance frequencies remain basically the same. Slight and random shifts, especially of the second peak, may be due to the different "packaging" of the tubes.
The constructive difficulty in making such small tubes can be overcome with similar remedies, such as the addiction of grid inserts inside the neck.

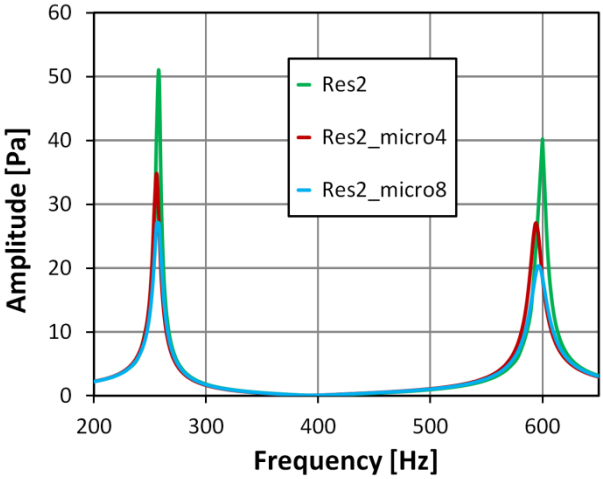

Figure 17: Effect of resonators with neck divided in a bundle of multiple tubes.

6 DOUBLE RESONATORS

Further developments in the use of resonators in piping are related to the tuning of multiple resonators for the elimination of many resonance peaks [27].
Figure 18 shows a scheme of a double resonator with two spherical cavities mounted in series at the end of the reference branch. Figure 19 shows the results that can be obtained with this device, the sizes of the double resonator are reported in Table VI. The previously described damping and de-tuning effects take place for the two resonance peaks of the side branch, occurring at 429 and 1287 Hz respectively.

Table VI: Dimensions of the double resonator.

l_1 $[m]$	d_1 $[m]$	V_1 $[m^3]$	l_2 $[m]$	d_2 $[m]$	V_2 $[m^3]$
0.0745	0.015	3.35E-5	0.008	0.015	1.67E-5

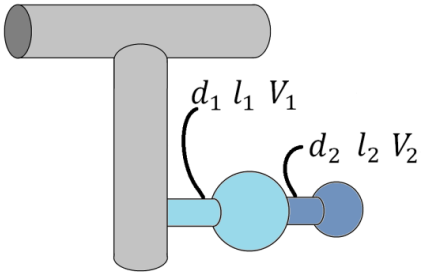

Figure 18: Scheme of a double resonator applied to the branch.

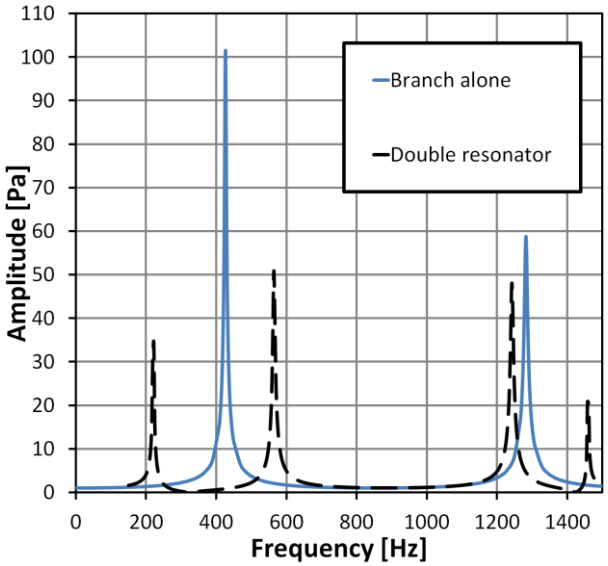

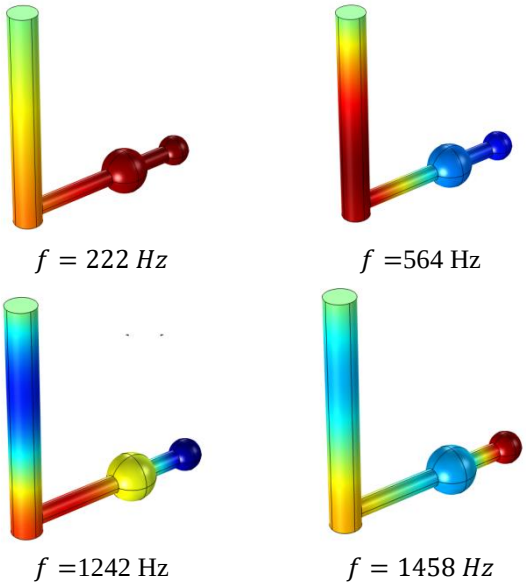

$f = 222\ Hz$ f =564 Hz

f =1242 Hz $f = 1458\ Hz$

Figure 19: Effect of a double resonator with the pressure contour plots at the new resonances (red maximum positive pressure, blue maximum negative pressure).

The first mode of the side branch, which is the 1/4 wave-length mode, is substituted by a mode at 222 Hz showing the largest pressure oscillations inside the double resonator, and

by a mode at 564 Hz with the side branch and the double resonator oscillating in opposition.
In both these modes the pressure oscillations inside the two cavities of the double resonator are in phase.
The second mode of the side branch, which is the 3/4 wave-length mode, is substituted by a mode at 1242 Hz with the end of the side branch and the second resonator oscillating in opposition, and by a mode at 1458 Hz chiefly involving the resonator with pressure oscillations of the two cavities in opposition. According to the diagram in Figure 3 the four new peaks correspond to flow velocities of 14, 36, 77 and 85 m/s. Therefore, there is a smaller distance between the critical speeds related to the second mode of the branch than between the critical speeds related to the first mode.
It is worth noticing that the interval between the first two critical speeds generated by the double resonator is similar to the one caused by a simple resonator with the same neck and cavity.

7 DISCUSSION AND CONCLUSIVE REMARKS

The aero-acoustic coupling mechanism that leads to FIV was presented by means of the critical speed chart. Several numerical simulations were then carried out in order to evaluate possible advantages of applying Helmholtz resonators to T-junctions with resonant side-branches. First, a sensitivity analysis was carried out to analyse the influence of the geometry and position of the resonator on the acoustic modes and critical speeds of the side branch. By modifying the geometry of the resonator it is possible to find both design solutions that cause large shifts of the critical speeds of FIV, and design solutions that generates smaller shifts of the critical speeds of FIV, but lead to large increases in damping.
The position of the resonator has a small influence on the amplitude and on the frequency of the resonance peaks as long as the resonator is located near the closed end of the side branch.
The results presented in this paper refer to a small size side branch, but in actual industrial applications the size of components may be rather larger. On the one hand, the coupling parameter of the resonator with an acoustic mode [8] depends on the modal shape and on the ratio between resonator volume and pipe volume, hence, the results can be extended to larger size systems with different natural frequencies provided that the modal shape does not change and that the ratio between volumes is kept constant. On the other hand, the losses in the piping system and in the resonator depends on many phenomena (e.g. radiation and viscous-thermal losses) which are influenced by the size of components and by frequency. Therefore, a careful analysis of these phenomena has to be carried out to extend results to different size systems.
The possibility of developing resonators with modified neck in order to improve damping was numerically analysed. Results show that both resonators with helical neck and resonators with the neck made up of a bundle of narrow ducts are able to significantly increase damping.
Numerical simulations also showed the potentialities of a double resonator that is able to dampen and de-tune two acoustic modes of a side branch.

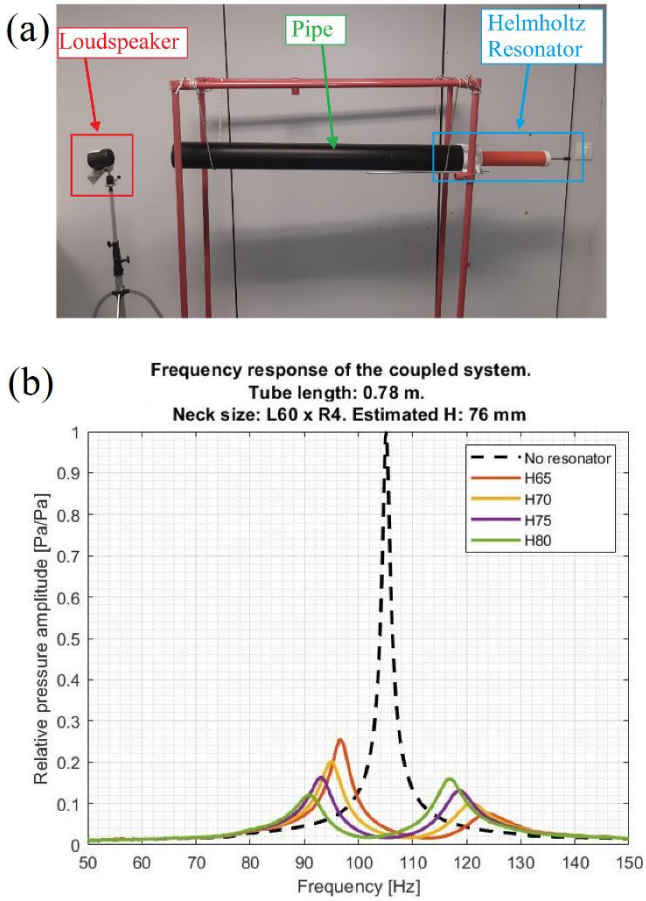

Figure 20: The testing rig (a) and experimental results (b).

In order to validate numerical results, a testing rig for resonators is being developed, see Figure 20. It is composed of a pipe (diameter 0.102 m, length 0.78 m) open at one end and closed at the other end and of a resonator with adjustable sizes. Excitation is performed by means of a loudspeaker placed outside the pipe and sound pressure is measured by means of microphones. Some preliminary results showed the appearance of minor resonance peaks that substitute for the original resonance peak of the pipe and the effect of the resonator's cavity volume on tuning.

NOMENCLATURE

c_0	$[m/s]$	Speed of sound in the medium
V_m	$[m/s]$	Mean velocity in main pipe
D_{mp}	$[m]$	Diameter of main pipe
d_{sb}	$[m]$	diameter of side branch
l_{sb}	$[m]$	length of side branch
Str	$[-]$	Strouhal number
f_v	$[Hz]$	Vortex shedding frequency

f_n	$[Hz]$	Natural acoustic frequencies of a side branch
d_{neck}	$[m]$	Diameter of the neck of a Helmholtz resonator
l_{neck}	$[m]$	Length of the neck of a Helmholtz resonator
D_{cavity}	$[m]$	Diameter of the cavity of a Helmholtz resonator
A_{neck}	$[m^2]$	Neck section Area of a Helmholtz resonator
V_{cavity}	$[m^3]$	Cavity volume of a Helmholtz resonator
f_{res}	$[Hz]$	Natural acoustic frequency of a Helmholtz resonator

REFERENCES

[1] Ziada S. and Lafon P., Flow-Excited Acoustic Resonance Excitation Mechanism, Design Guidelines, and Counter Measures. *Appl. Mech. Rev.*, Vol. 66, pp. 0108021-01080222, 2013.

[2] Tonon D., Hirschberg A., Golliard J. and Ziada S., Aeroacoustics of Pipe Systems With Closed Branches. *Int. J. Aeroacoust.*, Vol. 10(2), pp. 201–276, 2011.

[3] Ziada S. and Shine S., Strouhal Numbers of Flow-Excited Acoustic Resonance of Closed Side Branches. *J. Fluids Struct.*, Vol. 13, pp. 127–142, 1999.

[4] Xiao Y., Zhao W., Gu H., Zhang H. and Ghao X., Effects of branch length and chamfer on flow-induced acoustic resonance in closed side branches. *Ann. Nucl. Energy*, Vol. 121, pp.186–193, 2018.

[5] Bolduc M., Elsayed M. and Ziada S., Effect of Upstream Edge Geometry on the Trapped Mode Resonance of Ducted Cavities. *ASME PVP Conference*, Paris, France, Paper No. PVP2013-97149, 2013.

[6] Oshkay P., Velikorodny A., Flow acoustic coupling in coaxial side branch resonators with rectangular splitter plates. *Journal of Fluids and Structures*, Vol. 38, pp. 22-39, 2013.

[7] Tang P.K. and Sirignano W. A., Theory of a generalized Helmholtz resonator. *Journal of Sound and Vibration*, Vol. 26, pp. 247-262, 1973

[8] Fahy F.J. and Schofield C, A note on the interaction between a Helmholtz resonator and an acoustic mode of an enclosure. *Journal of Sound and Vibration*, Vol. 72, pp. 365-378, 1980.

[9] Doria A., Control of acoustic vibrations of an enclosure by means of multiple resonators. *J. of Sound and Vibration*, Vol. 181(4), pp. 673-685, 1995.

[10] Doria A., A simple method for the analysis of deep cavity and long neck acoustic resonator. *Journal of Sound and Vibration*, Vol. 232(4), pp. 823-833, 2000.

[11] Selamet A. and Lee I., Helmholtz resonator with extended neck. *The Journal of the Acoustical Society of America*, Vol. 114, pp. 1975-1985, 2003.

[12] Cai C., Mak C.M., Shi X., An extended neck versus a spiral neck of the Helmholtz resonator. *Applied Acoustics*, Vol. 115, pp. 74-80, 2017.

[13] Guan C., Jiao Z., Modeling and Optimal Design of 3 Degrees of Freedom Helmholtz Resonator in Hydraulic System. *Chinese Journal of Aeroacoustics*, Vol. 25, pp. 776-783, 2012.

[14] Xu M.B., Selamet A., Kim H., Dual Helmholtz resonator. *Applied Acoustics*, Vol. 71, pp. 822-829, 2010.

[15] Danneman M., Kucher M., Kunze E., Modler N., Knobloch K., Enghardt L., Sarradj E. and Höschler K., Experimental Study of Advanced Helmholtz Resonator Lines with Increased Acoustic Performance by Utilising Material Damping Effects. *Applied Sciences*, Vol. 8, 1923, 2018.

[16] Wang J., Rubini P., Qin Q. and Houston B., A Model to Predict Acoustic Resonant Frequencies of Distributed Helmholtz Resonators on Gas Turbine Engines. *Applied Sciences*, Vol. 9, 1419, 2019.

[17] Li L.,Liu Y., Zhang F. and Sun Z., Several explanations on the theoretical formula of Helmholtz resonator. *Advanced in Engineering Software*, Vol. 114, pp. 361-371, 2017.

[18] Cai C., Mak C.M., Noise attenuation capacity of a Helmholtz resonator. *Advances in Engineering Software*, Vol 116, pp. 60-66, 2018.

[19] Xiao Y., Gu H., Gao X., Zhang H. and Zhao W., Flow visualization study of flow induced acoustic resonance in closed side branches. *Ann. Nucl. Energy*, Vol. 120, pp. 559–568, 2018.

[20] Tonon D., Willems J.F.H. and Hirschberg A., Self-sustained oscillations in pipe systems with multiple deep side branches: Prediction and reduction by detuning. *Journal of Sound and Vibration*, Vol. 330, pp. 5894-5912, 2011.

[21] Oshkai P., Yan T., Velikorodny A. and VanCaeseele S., Acoustic power calculation in deep cavity flows: a semiempirical approach. *Journal of Fluids Engineering*, Vol. 130, pp. 1-9, 2008.

[22] Velikorodny A., Yan T., Oshkai P., Quantitative imaging of acoustically coupled flows over symmetrically located side branches. *Exp. Fluids*, Vol. 48, pp. 245–263, 2010.

[23] Kriesels P.C., Peters M.C.A.M., Hirschberg A., Wijnands A.P.J., Iafrati A., Riccardi G., Piva R. and Bruggeman J.C., High amplitude vortex-induced pulsations in a gas transport system. *Journal of Sound and Vibration*, Vol. 184, pp. 343-368, 1995.

[24] Vance J.M., *Rotodynamics of Turbomachinery*. J. Wiley & Sons, N. York, 1988.

[25] Bies D.A. and Hansen C.H., *Engineering Noise Control: Theory and Practice*, E&FN Spon, 2nd edn, 1996.

[26] Chen Y., Lee B. and Park Y., A Helmholtz Resonator with Spiral Neck for Analyte Concentration

Measurement in Low Frequency Range. *Appl. Sci.*, Vol. 10, 3676, 2020.

[27] Cossalter V., Doria A. and Gardonio P., Design and Testing of a Double Acoustic Resonator. *Machine Vibration*, Vol. 4, pp. 92-97, 1995.

ACKNOLEDGEMENT

This research was partially carried out in the framework of the PhD project: “FIV in piping”.